

References and Notes

- S. C. Brassell, G. Eglinton, I. T. Marlowe, U. Pflaumann, M. Sarnthein, *Nature* **320**, 129 (1986).
- F. G. Prahl, L. A. Muehlhausen, D. L. Zahnle, *Geochim. Cosmochim. Acta* **52**, 2303 (1988).
- $U_{37}^* = [C_{37:2}]/([C_{37:2}] + [C_{37:3}])$, where $[C_{37:2}]$ and $[C_{37:3}]$ are concentrations of C_{37} alkenone and alkatrienone, respectively (2).
- F. Rostek *et al.*, *Nature* **364**, 319 (1993).
- J.-C. Duplessy *et al.*, *Nature* **320**, 350 (1986).
- I. N. McCave, *Philos. Trans. R. Soc. London Ser. B* **348**, 229 (1995).
- L. D. Keigwin, B. H. Corliss, E. R. M. Druffel, E. P. Laine, *Quat. Res.* **22**, 383 (1984).
- L. D. Keigwin, G. A. Jones, *J. Geophys. Res.* **99**, 12397 (1994).
- J. P. Sachs, S. J. Lehman, *Science* **286**, 756 (1999).
- L. D. Keigwin, G. A. Jones, *Deep-Sea Res.* **36**, 845 (1989).
- J. F. Adkins, E. A. Boyle, L. D. Keigwin, E. Cortijo, *Nature* **390**, 154 (1997).
- Standard techniques of calibration (33) were used to express the *G. ruber* ages in calendar yr B.P., assuming a constant reservoir age of 350 ± 40 calendar years for surface ocean dissolved inorganic carbon (DIC) at this site (40). Model ages were assigned based on these results and on prior observations (7, 8, 10).
- The cores were correlated based on foraminiferal ^{14}C ages and % $CaCO_3$ profiles, as well as comparison with literature data (10, 24). For the ^{14}C measurements in core BC9, multiple subcores were correlated using % $CaCO_3$, and selected horizons were combined to yield sufficient alkenones for analysis. Alkenones were isolated as a compound class using a protocol described in detail by Ohkouchi *et al.* (47). Briefly, dried sediments were Soxhlet-extracted (ratio of methanol to dichloromethane, 3:7 v/v). The total lipid extract was saponified (using 0.5 M potassium hydroxide in methanol), and the neutral fraction was further separated into subfractions by silica gel column chromatography. A fraction containing alkenones was urea-adducted to separate straight chain compounds (including the alkenones) from branched and cyclic compounds. Polyunsaturated ketones were separated by argentation column chromatography, and a second silica gel column chromatographic step was used to remove remaining impurities. The resulting fraction contained only C_{36} - C_{39} alkenones with estimated purities consistently >95%. The purified alkenones were transferred to quartz tubes, vacuum-sealed with 100 mg of CuO , and combusted. The CO_2 produced was recovered and purified by cryogenic distillation and reduced to graphite over a cobalt catalyst (42). A small aliquot was used for measurement of $\delta^{13}C$. ^{14}C measurements were performed using methods for accurate determination of $^{14}C/^{12}C$ ratios in small samples at the National Ocean Science Accelerator Mass Spectrometry Facility (43).
- L. Fok-Pun, P. D. Komar, *J. Foram. Res.* **13**, 60 (1983).
- E. Bard, *Paleoceanography* **16**, 235 (2001).
- N. Ohkouchi, T. I. Eglinton, unpublished data.
- W. G. Mook, J. van der Plicht, *Radiocarbon* **41**, 227 (1999).
- E. P. Laine, C. D. Hollister, *Mar. Geol.* **39**, 277 (1981).
- D. O. Suman, M. P. Bacon, *Deep-Sea Res.* **36**, 869 (1989).
- D. J. W. Piper, D. A. V. Stow, W. R. Normark, in *Submarine Fans and Related Turbidite Systems*, A. H. Bouma, W. R. Normark, N. E. Barnes, Eds. (Springer, New York, 1985), pp. 137-142.
- W. J. Schmitz, M. S. McCartney, *Rev. Geophys.* **31**, 29 (1993).
- W. D. Gardner, L. G. Sullivan, *Science* **213**, 329 (1981).
- P. P. E. Weaver, R. G. Rothwell, J. Ebbing, D. Gunn, P. M. Hunter, *Mar. Geol.* **109**, 1 (1992).
- L. D. Keigwin, *Science* **274**, 1504 (1996).
- _____, R. S. Pickart, *Science* **286**, 520 (1999).
- J. F. Adkins, E. A. Boyle, L. D. Keigwin, *Eos* **76**, 282 (1995).
- R. G. Keil, E. Tsamakidis, B. Fuh, C. Giddings, J. I. Hedges, *Geochim. Cosmochim. Acta* **58**, 879 (1994).
- M. H. Conte, J. C. Weber, L. L. King, S. G. Wakeham, *Geochim. Cosmochim. Acta* **65**, 4275 (2001).
- Ocean Climate Laboratory, *World Ocean Atlas, 1998* (National Oceanographic Data Center, Silver Spring, MD, 1999) [CD ROM].
- W. L. Balsam, F. W. McCoy Jr., *Paleoceanography* **2**, 531 (1987).
- R. S. Bradley, P. D. Jones, Eds., *Climate Since A.D. 1500* (Routledge, London, revised ed., 1995).
- S. R. O'Brien *et al.*, *Science* **270**, 1962 (1995).
- M. Stuiver, P. J. Reimer, T. F. Braziunas, *Radiocarbon* **40**, 1127 (1998).
- Initial $\Delta^{14}C = (\Delta^{14}C_{meas} + 1) \exp(\lambda_p \tau) - 1$, where $\Delta^{14}C_{meas} = \exp(-\lambda_L t - \lambda_p \Delta t) - 1$; $\lambda_p = \ln 2/5730$ year $^{-1}$; $\lambda_L = \ln 2/5568$ year $^{-1}$; τ = time interval between deposition and measurement in calendar years (= model age + Δt , because model age refers to time before 1950); t = conventional radiocarbon age in radiocarbon years; and $\Delta t = 51$ calendar years, the time interval between 1950 and the measurement (17). Expression of $\Delta^{14}C$ in ‰ units implies multiplication by 1000.
- P. P. E. Weaver *et al.*, *Paleoceanography* **14**, 336 (1999).
- A. Benthein, P. J. Muller, *Deep-Sea Res. I* **47**, 2369 (2000).
- G. Mollenhauer *et al.*, unpublished results.
- G. M. Henderson, N. C. Slowey, *Nature* **404**, 61 (2000).
- M. Ikehara *et al.*, *Geophys. Res. Lett.* **24**, 679 (1997).
- E. R. M. Druffel, *Science* **275**, 1454 (1997).
- N. Ohkouchi, L. Xu, C. M. Reddy, T. I. Eglinton, in preparation.
- A. Pearson, A. P. McNichol, R. J. Schneider, K. F. von Reden, *Radiocarbon* **40**, 61 (1998).
- K. F. von Reden, R. J. Schneider, A. P. McNichol, A. Pearson, *Radiocarbon* **40**, 247 (1998).
- We thank J. McManus, J. Sachs, J. Adkins, and G. Eglinton, for discussions; three anonymous reviewers for constructive criticism of an earlier version of this manuscript; D. Montluçon, E. Roosen, and National Ocean Sciences Accelerator Mass Spectrometry Facility staff for laboratory assistance; and NSF (grant OCE-9809624) and the Japanese Society for the Promotion of Science for financial support. This is Woods Hole Oceanographic Institution contribution no. 10820.

20 June 2002; accepted 27 September 2002

Published online 10 October 2002;

10.1126/science.1075287

Include this information when citing this paper.

Vibrational Transition Moment Angles in Isolated Biomolecules: A Structural Tool

F. Dong and R. E. Miller

Infrared spectroscopy is used extensively in the study of isolated biomolecules, but it becomes less useful as it is applied to systems of increasing complexity. Even if the individual vibrational bands can be resolved spectroscopically, their assignment becomes problematic when they are more closely spaced than can be determined using ab initio methods. We describe a method that helps to alleviate this difficulty by measuring the direction of the vibrational transition moment for each vibrational band. The molecules of interest (adenine and cytosine) are cooled to 0.37 kelvin in liquid helium nanodroplets and oriented in a large dc electric field. A polarized infrared laser is then used to determine the directions of the infrared transition moments relative to the permanent dipole moment. Comparisons with ab initio calculations provide detailed structural information, including experimental evidence for nonplanarity of adenine and three tautomers of cytosine.

One reason for the recent interest in the spectroscopic study of isolated biomolecules (1, 2) is that these results can be compared with ab initio theory, providing new and important insights into the structure and dynamics of these systems. Noncovalent interactions, including the intramolecular forces between different parts of a highly flexible biomolecule (3) and intermolecular (solvent) interactions in clusters (4), are also being studied in this way. In the latter case, the issue of how the solvent influences the conformational preferences of the molecule can also be addressed by making comparisons between the structures observed for the isolated molecule and those in the associated water clusters of varying size (5); intermolecular hydrogen

bonding interactions can often "strain" the molecule of interest into conformations that are not favorable for the isolated molecule (6).

Vibrational spectroscopy is used extensively in these studies, because it can provide detailed information on both the structure and dynamics of systems of modest complexity (1, 4, 7, 8). For larger systems that have multiple conformations, the problems associated with resolving and then assigning the observed vibrational bands become formidable. Although pump-probe methods have proven useful in separating spectra associated with different conformers (7), progress toward the study of more complex systems will ultimately be limited by the ability to assign the different vibrational bands.

Here, we discuss a method for measuring the direction of the transition moment for

Department of Chemistry, University of North Carolina, Chapel Hill, NC 27599, USA.

each vibrational band in a spectrum. In this way, the vibrational bands can be labeled with angles between 0° and 90° , aiding in their assignment. As shown below, these vibrational transition moment angles (VTMAs) are also extremely sensitive to the directionality of the bonds in the molecule, so that they provide detailed information on the structure. Because an N -atom molecule has $3N - 6$ vibrational degrees of freedom, the structural information contained in these VTMA scales with the molecule's size.

The experimental measurement of VTMA requires that the molecules of interest be oriented/aligned (9) in the laboratory frame of reference. The associated difficulties are substantial for isolated molecules, accounting for the lack of such data. For molecules solvated in a polymer, the desired alignment can be achieved by stretching the film. Alternatively, infrared (IR) spectroscopy can be carried out on molecular crystals, which provide the needed orientation (10). IR linear dichroism (11) can then be used to measure the difference between the vibrational band intensities for light polarized parallel and perpendicular to the alignment axis. Unfortunately, comparisons between experiment and theory are complicated by the fact that the molecules are not isolated and the molecular orientation is somewhat ill-defined (9, 12).

We present a method for determining VTMA for isolated molecules, applied here

to the study of nucleic acid bases. The molecules of interest are isolated in liquid helium nanodroplets (13–16), which cool the molecules to very low temperature (0.37 K) (17) and are so weakly interacting that the associated IR spectra can be compared directly with *ab initio* calculations. The present method can also be applied to gas-phase studies, provided that the temperature is comparably low, such that a dc electric field can be used to orient the dipole moment of the molecule (18). With the dipole moment of the molecule oriented in the laboratory frame, the VTMA (defined here as the angles between the permanent dipole moment and the vibrational transition moment directions) can be obtained from measurements of the relative intensities of the vibrational bands with the laser polarized parallel and perpendicular to the dc field.

The IR spectrum of adenine solvated in He (Fig. 1) reveals three clearly resolved bands, corresponding to the N-H, NH_2 symmetric (SS), and NH_2 asymmetric (AS) stretches (19). In the structure of adenine (Fig. 1), the arrow indicates the direction of the calculated permanent dipole moment. This spectrum is in excellent agreement with that obtained in a recent gas-phase study using IR-ultraviolet double-resonance spectroscopy (19). The assignment of this spectrum is quite straightforward, given that the vibrational bands are widely separated. In-

deed, *ab initio* frequencies [MP2/6-311G** with Gaussian98 (20)], scaled by a factor of 0.953 (to account for anharmonicity), give a convincing assignment, as indicated by the vertical arrows in Fig. 1. Even here, the differences between the experimental and calculated frequencies are significant.

At the cold temperature of the helium droplets, substantial orientation of the adenine can be achieved with experimentally realizable dc electric fields (52 kV/cm) (13, 21). The F-center laser used here is linearly polarized, and the laser field can be aligned parallel or perpendicular to the dc field. For a vibrational mode with its transition moment parallel to the permanent dipole moment, alignment of the laser electric field parallel to the dc field enhances the band intensity as the transition moment becomes better aligned with the laser electric field; conversely, alignment of the laser electric field perpendicular to the dc field diminishes the band intensity as the transition moment becomes more poorly aligned with the laser electric field. Alternatively, if the transition moment is perpendicular to the permanent dipole moment, a dc field-induced enhancement will occur when the laser is polarized perpendicular to the dc field. Intermediate angles will result in more muted effects.

Expanded spectra of the three vibrational bands of adenine are shown in Fig. 2, recorded under field-free, parallel, and perpendicular (orientation of the dc field relative to the laser electric field) polarization conditions. Each band displays a distinct behavior, depending on the laser polarization direction. Qualitatively, the NH_2 (AS) is enhanced by a parallel field, and the NH_2 (SS) becomes stronger upon application of a perpendicular field. The N-H stretch only weakly depends on the field, which suggests that its associated VTMA is near the magic angle, namely 54.7° (9).

The results in Fig. 2 can be used to determine VTMA in a manner similar to that of Kong (18) for the electronic TMAs. The orientation distribution for the permanent dipole was calculated at the experimental electric field strength (52 kV/cm) and a rotational temperature of 0.37 K, determined by evaporative cooling of the helium droplets. Because the present spectra are not rotationally resolved, *ab initio* rotational constants [reduced by a factor of 3 to account for the effects of the helium (22)] were used in the calculations of the orientation distribution. At the electric fields used in the present experiments, the calculated distribution is rather insensitive to the magnitudes of the rotational constants. Indeed, a factor of 2 change in the rotational constants (much larger than the expected uncertainty) results in a variation in the VTMA of less than 5° . The results are similarly insensitive to the magnitude of the permanent dipole moment, which is also tak-

Fig. 1. IR spectrum of adenine in the liquid helium droplets. The vertical arrows indicate *ab initio* frequencies (MP2/6-311G**), scaled by a factor of 0.953 (needed to bring the calculated harmonic N-H stretch frequency into agreement with the experimental value). The inset shows the most stable isomer of adenine. The arrow indicates the direction of permanent dipole moment.

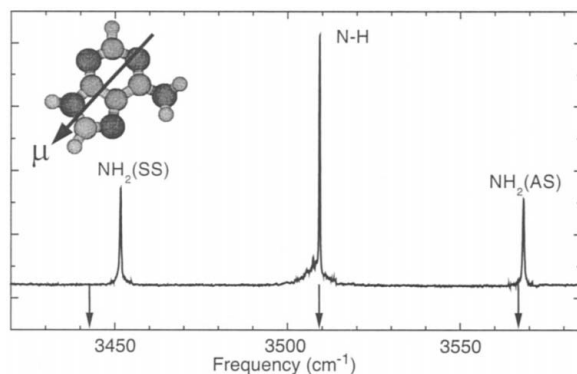
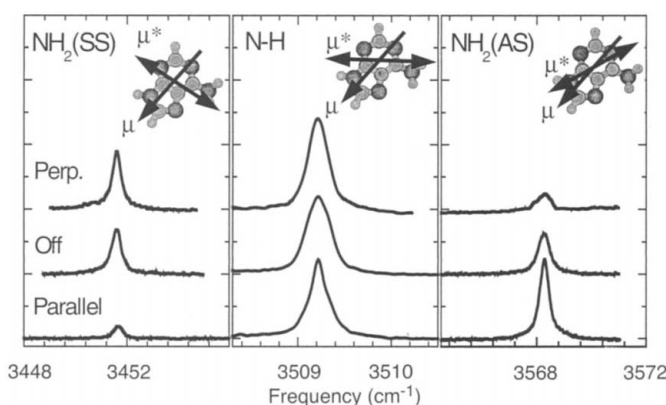


Fig. 2. Expanded IR spectra of the three vibrational bands of adenine under parallel polarization, zero dc field (Off), and perpendicular polarization (Perp.) conditions. Parallel and perpendicular refer to the angle between the laser electric field and the applied dc field (52 kV/cm). The permanent dipole directions and transition moment directions are superimposed on the inset structures, which are labeled as μ and μ^* , respectively



REPORTS

en from ab initio calculations. The dipole distribution function was then used to calculate the ratio of the parallel to perpendicular (integrated) band intensities for different values of the VTMA. The experimental ratios were used to determine the VTMA listed in Table 1.

The ab initio VTMA are also listed in Table 1, specifically those calculated with a moderately large basis set (MP2/6-311G**). The agreement between the experimental and calculated values is clearly excellent. Because large basis set ab initio calculations become prohibitively expensive for larger molecules, we carried out an extensive study of the dependence of the VTMA on the basis set, as shown in Fig. 3 for adenine. Note that the smallest basis set is no longer even considered reasonable for serious calculations, and yet the associated VTMA are reasonable. The inadequacies of these basis sets are more clearly illustrated by the large deviations in the vibrational frequencies, relative to those obtained with the larger basis sets. The VTMA are rather insensitive to basis set for the high-frequency (local) vibrations considered here, because they are primarily determined by bond directionality and do not depend strongly on the detailed force fields. Therefore, provided the overall molecular structure is accurately reproduced, the directions of the permanent and transition moments will be well determined. Note that no scale factors are required for the calculated VTMA, compared to experiment. In contrast, the harmonic vibrational frequencies not only are highly sensitive to basis set size but also are poor approximations to the experimental (anharmonic) results.

The applicability of density functional theory (DFT) to the calculation of VTMA is important to understand, given the interest in extending these methods to larger systems. In the process of exploring this aspect of the problem, it became clear just how sensitive these VTMA are to the molecular structure. To illustrate this point, we note that the MP2 calculations presented above, which agree quantitatively with the experimental results, give a non-planar adenine structure, corresponding to the NH₂ group being tilted out of plane by ~20° (23). In contrast, a full geometry optimization at the DFT [B3LYP/6-311++G(d,p)] level yielded an essentially planar structure and a set of VTMA in poor agreement with experiment (see Table 1). In particular, the DFT VTMA for the NH₂(AS) mode is much smaller than the experimental value. MP2 calculations were also performed with the molecule constrained to be planar, resulting in similar errors in the VTMA. Indeed, the only calculations that reproduced the experimental results were those that gave the out-of-plane tilted structure. These results provide convincing experimental evidence in support of the nonplanar structure

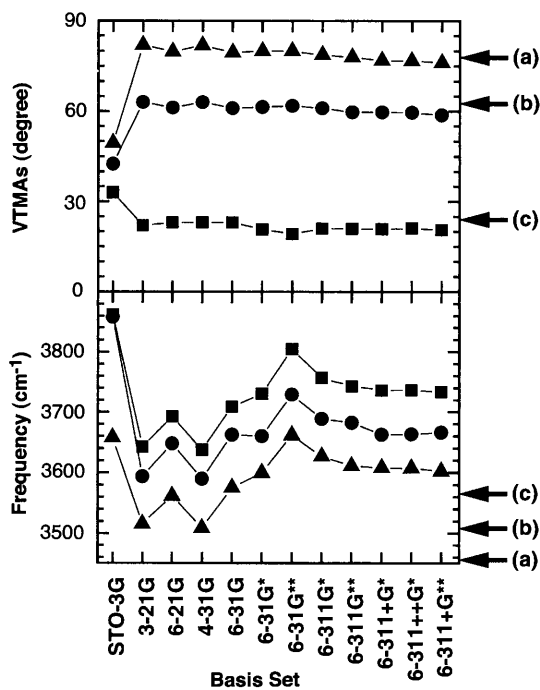


Fig. 3. Basis set dependence of the vibrational frequencies (lower panel) and VTMA (upper panel) for the three modes of adenine [squares, NH₂(AS); circles, N-H stretch; triangles, NH₂(SS)] shown in Figs. 1 and 2 (at the MP2 level). The horizontal arrows indicate the experimental frequencies and VTMA [(a), NH₂(SS); (b), N-H stretch; (c), NH₂(AS)]. Note that even for the large basis sets, there is a large difference between the experimental and calculated frequencies, which is largely the result of anharmonicity.

Table 1. Experimental (Exp.) and ab initio (Calc.) VTMA (in degrees) and frequencies (in wavenumbers) for adenine and cytosine. The ab initio frequencies have been scaled at a factor of 0.953 (see text). With the exception of the DFT calculation (B3LYP/6-311++G**) for adenine, all calculations were performed at the MP2/6-311G** level of theory.

Molecule		NH ₂ (SS)		NH ₂ (AS)		X-H (X = N,O)	
		Exp.	Calc.	Exp.	Calc.	Exp.	Calc.
Adenine	Freq.	3451.63	3441.6	3568.25	3567.0	3509.23*	3509.0*
	VTMA (MP2/DFT)	77	78/82	24	21/3	63*	60/69*
Cytosine (keto)	Freq.	3451.64	3442.2	3572.63	3743.4	3471.68*	3485.6*
	VTMA	85	88	7	6	76*	78*
Cytosine (cis-enol)	Freq.	3455.92	3443.1	3572.33	3564.2	3609.75†	3665.1†
	VTMA	68	68	26	27	48†	45†
Cytosine (trans-enol)	Freq.	3457.30	3442.9	3570.97	3737.3	3617.66†	3671.2†
	VTMA	28	28	62	66	80†	90†

*N-H stretch. † O-H stretch.

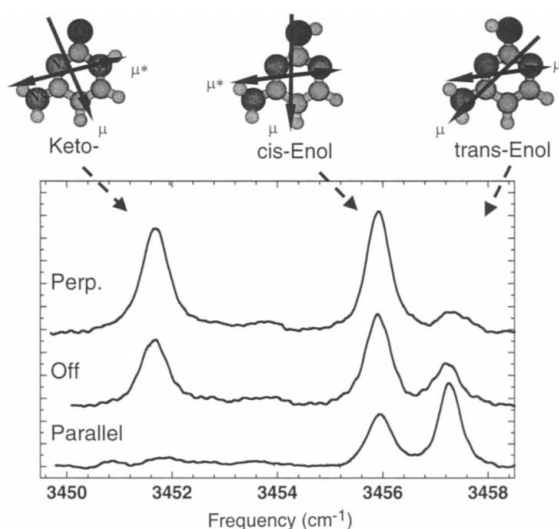


Fig. 4. IR spectra and assignments of NH₂(SS) vibrations of cytosine tautomers under parallel polarization, zero field, and perpendicular polarization conditions. The permanent dipole directions and transition moment directions are superimposed on the inset structures, which are labeled as μ and μ^* , respectively.

obtained from the MP2 calculations (23). Earlier microwave studies revealed that adenine has a large inertial defect (24). Although this is consistent with our results, it does not uniquely determine the source of the nonplanarity.

The simplicity of the above spectrum results from the relatively small size of the molecule and the fact that there is only a single isomer of adenine produced by thermal evaporation. In contrast, cytosine is known to have a number of low-energy isomeric forms (25). Although it is well established that there are at least keto and enol forms of cytosine, there is still some uncertainty regarding which form(s) of the latter can be observed (26). As shown in Fig. 4, two different enol forms have been proposed (25), associated with the directionality of the O-H bond.

The spectrum of the NH₂(SS) region of cytosine (solvated in He droplets) is shown in Fig. 4. It consists of three bands, even though a single isomer of cytosine would only have a single band in this spectral region. The implication is that there are three isomers of cytosine present in the He droplet environment. Nonetheless, an unambiguous assignment of these bands on the basis of the vibrational frequencies alone is difficult, given their small spacing relative to the accuracy of the corresponding ab initio calculations. It is evident from Fig. 4 that the field dependences of these three bands are distinctly different. When compared with the ab initio VTMA's for the various isomers of cytosine (Table 1), the assignment of the spectrum becomes clear. Namely, in order of increasing vibrational frequency, the bands are assigned to the keto, cis-enol, and trans-enol isomers. Further evidence in support of this assignment comes from the other X-H stretches of these isomers (Table 1). In all cases, there is excellent agreement between the experimental and calculated VTMA's.

The largest deviation (10°) occurs for the trans-enol O-H stretch, which could be an indication of mode coupling in this case, although the signal-to-noise ratio for this band is rather low, making the data somewhat less accurate. It is noteworthy that the assignment based on the VTMA's puts the cis-enol isomer at a slightly lower frequency than the trans-enol form, which is exactly the opposite of the ab initio prediction. Indeed, the frequencies for these two isomers are so similar as to preclude an assignment based on the frequencies alone. Indeed, these two bands were not even resolved in the previous argon matrix isolation study of this system (26).

Our results for adenine show that the molecule is nonplanar, with the NH₂ group tilted ~20° out-of-plane. As pointed out elsewhere (27), it was generally believed (28) that nucleic acid bases were planar, or at least that the biological consequences of nonplanarity were weak. This point of view changed with

the observation of abundant interstrand amino-group contacts in B-DNA crystal structures, which appear to be stabilized by amino-group pyramidalization and interstrand bifurcated hydrogen bonds (27). Although the ab initio calculations provide considerable evidence for the nonplanarity of the bases, it was noted in 1999 that "clear, direct experimental evidence about the nonplanarity of isolated bases is still missing due to the resolution of the available experimental techniques" (27). This situation has now changed and it will be interesting to study other systems, including guanine, for which ab initio calculations suggest the out-of-plane angle is anomalously large (27).

The results reported here for cytosine show how VTMA's can also be used to assign complex spectra arising from the presence of multiple tautomers. The method will be particularly useful in the study of water clusters with biomolecules, where the location of the water molecule can easily be determined by recording the VTMA's for the corresponding H-bonded and free O-H stretching vibrations. It is also encouraging that the number of VTMA's increases with the number of atoms in the molecule (3N - 6 in principle), so that more structure information is available for the larger systems where it is needed most.

References and Notes

1. B. C. Dian, A. Longarte, T. S. Zwier, *Science* **296**, 2369 (2002).
2. D. W. Pratt, *Science* **296**, 2347 (2002).
3. D. R. Borst, J. R. Roscioli, D. W. Pratt, *J. Phys. Chem. A* **106**, 4022 (2002).
4. T. S. Zwier, *J. Phys. Chem. A* **105**, 8827 (2001).
5. L. C. Snoek, R. T. Kroemer, J. P. Simons, *Phys. Chem. Chem. Phys.* **4**, 2130 (2002).
6. A. Dkhissi et al., *J. Phys. Chem. A* **104**, 9785 (2000).
7. E. Nir et al., *Phys. Chem. Chem. Phys.* **4**, 732 (2002).
8. M. Mons et al., *J. Phys. Chem. A* **106**, 5088 (2002).
9. J. Michl, E. W. Thulstrup, *Spectroscopy with Polarized Light: Solute Alignment by Photoselection in Liquid*

Crystals, Polymers, and Membranes, (VCH, Weinheim, Germany, 1995), pp. 150-189.

10. D. Marsh, M. Müller, F.-J. Schmitt, *Biophys. J.* **78**, 2499 (2000).
11. A. Holmén, *J. Phys. Chem. A* **101**, 4361 (1997).
12. J. G. Radziszewski et al., *J. Am. Chem. Soc.* **118**, 10275 (1996).
13. K. Nauta, R. E. Miller, *Science* **283**, 1895 (1999).
14. K. K. Lehmann, G. Scoles, *Science* **279**, 2065 (1998).
15. Helium nanodroplets were formed by expanding high-purity helium gas from 60 atm through an orifice 5 μm in diameter (cooled to ~23 K) into vacuum, resulting in a beam of droplets with a mean diameter of ~3 nm (~3000 atoms). These droplets passed through an oven containing a low vapor pressure (between 10⁻⁶ and 10⁻⁵ torr) of the nucleic acid base of interest. The gas-phase molecules were captured and solvated by the droplets when collisions between them occurred. The seeded droplets then passed through an IR laser [an F-center laser (16)], where the solvated molecule was vibrationally excited. Relaxation of the excited molecule led to the evaporation of several hundred He atoms and caused a depletion of the droplet beam, which was detected with a bolometer (16). The IR spectrum was obtained by scanning the laser through the various vibrational bands and recording the laser-induced decrease in the He droplet beam intensity.
16. R. E. Miller, *Science* **240**, 447 (1988).
17. M. Hartmann, R. E. Miller, J. P. Toennies, A. F. Vilesov, *Phys. Rev. Lett.* **75**, 1566 (1995).
18. W. Kong, *Int. J. Mod. Phys. B* **15**, 3503 (2001).
19. C. Plützer, E. Nir, M. S. De Vries, K. Kleinermanns, *Phys. Chem. Chem. Phys.* **3**, 5466 (2001).
20. M. J. Frisch et al., *Gaussian 98* (Gaussian, Pittsburgh, PA, 1998).
21. K. Nauta, D. T. Moore, P. L. Stiles, R. E. Miller, *Science* **292**, 481 (2001).
22. C. Callegari, K. K. Lehmann, R. Schmied, G. Scoles, *J. Chem. Phys.* **115**, 10090 (2001).
23. S. K. Mishra, M. K. Shukla, P. C. Mishra, *Spectrochim. Acta A* **56**, 1355 (2000).
24. J. S. Kwiatkowski, R. J. Bartlett, W. B. Person, *J. Am. Chem. Soc.* **110**, 2353 (1988).
25. P. Ü. Civcir, *J. Mol. Struct. (Theochem.)* **532**, 157 (2000).
26. M. Szczesniak et al., *J. Am. Chem. Soc.* **110**, 8319 (1988).
27. P. Hobza, J. Sponer, *Chem. Rev.* **99**, 3247 (1999).
28. S. Kawahara, T. Uchimaru, K. Taira, M. Sekine, *J. Phys. Chem. A* **106**, 3207 (2002).
29. Supported by NSF grant CHE-99-87740. We thank W. Kong for providing the program for calculating the orientation distributions.

2 August 2002; accepted 9 October 2002

Sperm-Female Coevolution in *Drosophila*

Gary T. Miller and Scott Pitnick*

Rapid evolution of reproductive traits has been attributed to sexual selection arising from interaction between the sexes. However, little is known about the nature of selection driving the evolution of interacting sex-specific phenotypes. Using populations of *Drosophila melanogaster* selected for divergent sperm length or female sperm-storage organ length, we experimentally show that male fertilization success is determined by an interaction between sperm and female morphology. In addition, sperm length evolution occurred as a correlated response to selection on the female reproductive tract. Giant sperm tails are the cellular equivalent of the peacock's tail, having evolved because females evolved reproductive tracts that selectively bias paternity in favor of males with longer sperm.

Male reproductive traits appear to evolve more rapidly than other types of character (1). For example, DNA sequence comparisons

reveal that male-derived molecules involved in reproduction exhibit a high level of divergence among members of the primate lineage